

# What Is the Difference between the Manganese Porphyrin and Corrole Analogues of Cytochrome P450's Compound I?

Sam P. de Visser,<sup>[a]</sup> François Ogliaro,<sup>[a]</sup> Zeev Gross,<sup>\*,[b]</sup> and Sason Shaik<sup>\*,[a]</sup>

**Abstract:** Density functional calculations on oxo-manganese complexes of corrole (**1**) and porphyrin (**2** and **3**) show a fundamental difference. The ground state of **1** is the singlet manganese(v) state,  $^1A(Mn^V)$ , in which corrole is a closed shell. In contrast, **2** and **3** have high-spin manganese(IV) states,  $^3A_{1u}$  and  $^3A_{2u}$ , respectively. This difference and the state ordering for each system are rationalized based on the competition

between the intrinsic tendency of manganese to prefer high-spin electronic configurations, vis-à-vis the general tendency to prefer double occupancy in the low-lying orbitals. The outcome of this

**Keywords:** density functional calculations • metalloenzymes • oxo-manganese corrole • oxomanganese porphyrin

competition is determined primarily by the identity of the macrocycle, corrole versus porphyrin. Corrole with a small cavity holds the MnO moiety with a high off-plane displacement, and thereby prefers the low-spin state. On the other hand, porphyrin with the wider cavity holds the MnO moiety closer to the plane, and thereby prefers high-spin states.

## Introduction

Cytochrome P450 constitutes a family of enzymes that are responsible for many catalytic reactions, involving both biodegradation and biosynthesis.<sup>[1]</sup> From a structural point of view, the common feature of all cytochrome P450 species is a cysteinate-coordinated iron(III) porphyrin placed within a cavity provided by the apo-protein. Most, albeit not all, of the catalytic reactions are considered to proceed through a high-valent (oxo)iron intermediate, the so-called Compound I. Compound I contains the oxygen atom that is ultimately transferred to the organic substrate. Despite enormous efforts, this active form of P450 has never been fully characterized. But, Compound I of the related horseradish peroxidase (HRP-I, histidine is coordinated to the metal) has been identified as an oxoiron(IV) porphyrin radical complex by many spectroscopic methods. These intriguing biochemical systems initiated the development of synthetic catalysts for

the selective oxidation of organic substrates under mild reaction conditions.<sup>[2, 3, 4]</sup>

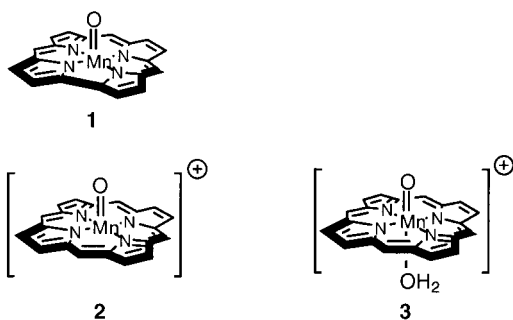
In the course of these investigations manganese porphyrins were found to be more potent catalysts than analogous iron complexes.<sup>[2a]</sup> Nevertheless, characterization of the active species of these manganese complexes has remained a formidable task for a very long time. A recent breakthrough was provided by Groves and co-workers, who have shown that positively charged *ortho*-pyridylum *meso* substituents stabilize the manganese(v) oxidation state in porphyrins ( $Mn^VO-Por$ ) to an extent that allows spectroscopic investigations.<sup>[2d, 2e, 2f]</sup> More recently, an (oxo)manganese(v) complex with a corrole ( $MnOCor$ ) rather than a porphyrin ring was synthesized by one of us and found to be relatively long-lived and of low oxygen-transfer reactivity.<sup>[5]</sup> In both  $Mn^VO-Por$  and  $Mn^VO-Cor$  systems, the diamagnetism of the complexes was used as the main support for the (oxo)manganese(v) assignment. Another important catalytic system that might proceed through (oxo)manganese(v) intermediates is that based on salen complexes.<sup>[6, 7]</sup>

The generation of corrole complexes provided an intriguing puzzle regarding the reactivity of  $Mn^VO-Por$  vis-à-vis  $Mn^VO-Cor$ . Thus, while the former epoxidizes olefins fast and efficiently, the latter was reported to be quite a sluggish oxidant. The reason for this intriguing pattern is unclear and its understanding is important and once achieved, may serve as means to design better oxidation catalysts.

To gain insight into the nature of the (oxo)manganese(v) moiety in synthetic and biological catalysts, we decided to study the oxomanganese corrole [ $MnOCor$ ] (**1**) and compare

[a] Prof. S. Shaik, Dr. Sam.P. de Visser, Dr. F. Ogliaro  
Department of Organic Chemistry and  
The Lise Meitner-Minerva Center for Computational Quantum  
Chemistry  
The Hebrew University of Jerusalem, 91904 Jerusalem (Israel)  
Fax: (+972)2-6584680  
E-mail: sason@yfaat.ch.huji.ac.il

[b] Prof. Z. Gross  
Department of Chemistry and Institute of Catalysis  
Science and Technology  
Technion, Haifa 32000 (Israel)  
E-mail: chr10zg@technion.ac.il



its properties with the isoelectronic oxomanganese porphyrin cation  $[\text{MnOPor}]^+$  (**2**) and the hexacoordinate water complex  $[\text{MnOPorH}_2\text{O}]^+$  (**3**). One important difference between the porphyrin and corrole rings is that while corroles act as trianionic ligands (supplying a charge of  $3^-$ ), porphyrins are dianionic. Since the oxo ligand is counted as  $\text{O}^{2-}$ , five-coordinate  $\text{MnOCor}$  is neutral, whereas the corresponding porphyrin complexes are either positively charged or charge-balanced by an additional anionic ligand (*trans* to the metal-oxygen, to give a hexacoordinate complex).<sup>[8]</sup> To keep comparable spin states, the same oxidation states were investigated for both complexes. Water was chosen as a ligand for **3** because many of the synthetic catalysts may involve this weak ligand.<sup>[2b]</sup> The present results will be compared with our recent studies of iron-based Compound I<sup>[9]</sup> and with recent results by Ghosh et al. on metallocorrole systems.<sup>[10]</sup>

**Abstract in Dutch:** *De fundamentele verschillen tussen oxomangaan complexen met corrool (**1**) en porfyriene (**2** en **3**) zijn met behulp van dichtheidsfunctionaal berekeningen aange-toond. De grondtoestand van **1** is een singulet mangaan(v) toestand,  $^1\text{A}(\text{Mn}^{\text{V}})$ , waarin corrool een gesloten schil heeft. Complexen **2** en **3** daarentegen hebben een hoog-spin mangaan(IV) grondtoestand, respectievelijk  $^3\text{A}_{1u}$  en  $^3\text{A}_{2u}$ . Dit verschil tesamen met de toestandsvolgorde voor elk systeem is gerationaliseerd op de basis van de competitie tussen de intrinsieke voorkeur van mangaan voor hoog-spin electronische configuraties ten opzichte van de algemene voorkeur voor dubbel-bezetting van de laagliggende orbitalen. Het resultaat van deze competitie wordt voornamelijk bepaald door de identiteit van de macrocyclus, corrool ten opzichte van porfyriene. De MnO eenheid zit in de corrool groep ingesloten doch is sterk uit het vlak getild waardoor de laagspin toestand de voorkeur krijgt. Porfyriene daarentegen heeft de MnO eenheid dichtbij het vlak, wat de voorkeur geeft aan hoogspin toestanden.*

#### Abstract in Hebrew:

חישובי פונקציונל צפיפות על קומפלקסי אוקסו-מנגן של קורול (**1**) ופורפירין (**2** ו- **3**) מפינים הבדל יסודי. מצב היסוד של **1** הוא מצב הסינגלט בעל מנגן  $^1\text{A}(\text{Mn}^{\text{V}})$ , אשר בו טבעת הקורול היא סגורה – קליפה. בניגוד לכך, **2** ו- **3** הם בעלי מצבי יסוד גבוהי ספין של מנגן  $^3\text{A}_{1u}$  ו-  $^3\text{A}_{2u}$  בהתאמה. ההבדל הזה, וסדר המצבים האלקטרוניים הנמוכים נידון ומוסבר כתוצאה של התחרות בין הנטייה של מנגן להעדיף מצבים גבוהי ספין לעומת הנטייה הכללית להעדיף אכלוס כפול באורביטלים נמוכי אנרגיה. תוצאת התחרות הזאת מוכרעת על ידי זהות הטבעת המקרוציקלית, קורול לעומת פורפירין. קורול בעל המיפתח הקטן גורם להתרוממות המנגן מעל המישור ומעדיף על כן אכלוס בעל מצב נמוך ספין. לעומתו בפורפירין בעל המיפתח הגדול, המנגן קרוב יותר למישור ויש העדפה למצבים גבוהי ספין.

## Computational Methods

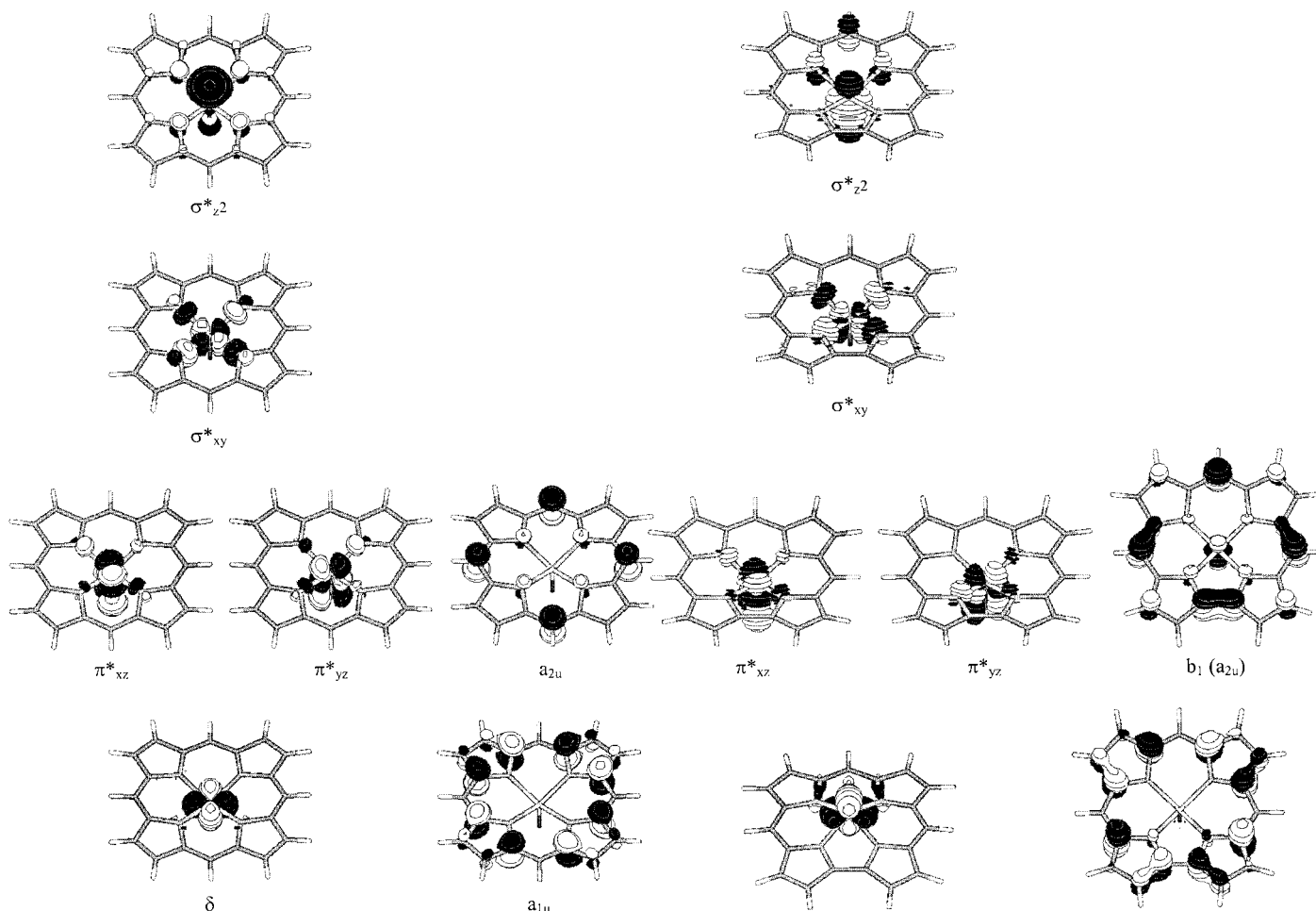
Quantum-chemical calculations were performed with the Jaguar 4.1 program package.<sup>[11]</sup> The hybrid density functional method UB3LYP with the double zeta quality LACVP basis set was used. The complexes were optimized in the three different relevant spin states, that is singlet, triplet, and quintet. Both ferro- and antiferromagnetic pairs were calculated wherever appropriate.

Density functional theory often yields incorrect ordering of spin states for transition metals. This arises especially in situations of  $s^1d^{n-1}$  versus  $d^n$  configurations (as, for example, in  $\text{Fe}^+$ ) for which it is now well documented that hybrid density functionals favor artificially the electronic configurations with high  $d$  population.<sup>[12]</sup> These deficiencies largely disappear in transition metal complexes in which the metal  $s$  orbital is not available anymore (due to its involvement in bonding orbitals which are invariably doubly occupied). Thus, unless one computes a process in which a metal or a metal ion is extruded, one can consider the state ordering to be reliable at least in a qualitative sense. In reactions of metal ion extrusion it is often sufficient to shift the energy level of the metal or metal ion as done, for example, in reference[13]. Another concern is the calculation of excited states, as done here. Our experience with a variety of transition metal species is that if a given orbital occupation scheme is maintained throughout the iterative procedure of orbital optimization, the results should be reliable, at least in a qualitative sense. This is so perhaps due to the strong local symmetry of the metal orbitals in an octahedral field. Finally, spin contamination is a problem in quantum chemistry. However, its energy aspects are less severe in density functional calculations. Furthermore, spin-projection techniques, which are widely used in molecular orbital calculations are less meaningful in density functional theory. The spin contamination in systems **1–3** is quite moderate and the relative energies can be assumed reliable. Caution along with detailed understanding of the electronic structure is a good recipe in any density functional calculations of transition metal species.

## Orbital Scheme and State Assignment

The highest lying occupied and lowest lying virtual molecular orbitals of  $[\text{MnOPor}]^+$  and  $\text{MnOCor}$  are schematically depicted in Scheme 1 and 2, respectively. The left-hand-side of Schemes 1 and 2 shows the set of five manganese  $d$  orbitals ( $\delta$ ,  $\pi_{xz}^*$ ,  $\pi_{yz}^*$ ,  $\sigma_{xy}^*$ , and  $\sigma_{z^2}^*$ , with the  $x$  and  $y$  axes passing through the *meso*-carbon atoms). Lowest lying is the non-bonding  $\delta$  orbital, followed by a virtually degenerate pair of  $\pi_{\text{MnO}}^*$  orbitals resulting from the interaction of the manganese  $d_{xz}$  and  $d_{yz}$  orbitals with the  $p_x$  and  $p_y$  atomic orbitals of oxygen. The highest lying and virtual orbitals are  $\sigma^*$  type, which are antibonding in the Mn–N linkages ( $\sigma_{xy}^*$ ) and in the Mn–O bond ( $\sigma_{z^2}^*$ ).

On the right-hand-side of Schemes 1 and 2, we present the two highest occupied porphyrin/corrole orbitals.<sup>[5, 10b]</sup> With 16 atoms in the macrocyclic periphery (discounting the  $\text{C}_\beta\text{--C}_\beta$  moieties of the pyrrole rings), porphyrin possesses an almost



Scheme 1. Key high-lying occupied and low-lying virtual orbitals of [MnOPor]<sup>+</sup>.

Scheme 2. Key high-lying occupied and low-lying virtual orbitals of MnOCor.

degenerate pair of orbitals. The symmetry labels  $a_{1u}$  and  $a_{2u}$  are for  $D_{4h}$  symmetry, but for convenience we use these labels also for the lower symmetry systems. With a CH group missing in corrole, the macrocyclic periphery of corrole has 15 atoms and also leads to a pair of virtually degenerate orbitals, designated as  $a_2$  and  $b_1$  in Scheme 2. These latter labels correspond to the  $C_{2v}$  symmetry of the complex, however, to keep the analogy with porphyrin<sup>[10b]</sup> we label them also as  $a_{1u}$  and  $a_{2u}$ .

## Results and Discussion

All optimized electronic states are presented in Tables 1–3, which provide relative energies, group spin densities, and critical bond lengths for the electronic states of optimized **1**, **2**, and **3**. The term symbols of the states are not related to the real state symmetry, but provide a commonly accepted nomenclature. Thus, all states that involve a

single-electron occupancy in  $a_{1u}$  and  $a_{2u}$  (Scheme 1) are symbolized by  $A_{2u}$  and  $A_{1u}$ , respectively, and for all the closed-shell states (e.g., Table 1, entry 1) and their excited states (e.g., Table 1, entry 9) we use plain A as the term symbol. In all cases we provide the manganese oxidation state<sup>[8]</sup> in parentheses and the spin multiplicity ( $2S+1$ ). Further information is provided by the orbital occupancy.

Although all the target species are isoelectronic, their ground states were found to exhibit substantial differences.

Table 1. State characterization, relative energies, group spin densities ( $\rho$ ), and critical bond parameters ( $r$ ,  $\Delta$ ) of MnOCor.<sup>[a]</sup>

Entry	Electronic configuration	Orbital occupancy	$E_{\text{rel}}$ [kcal mol <sup>-1</sup> ]	$\rho_{\text{Mn}}$	$\rho_{\text{O}}$	$\rho_{\text{Cor}}$	$r_{\text{MnO}}$	$r_{\text{MnN}}$ (average)	$\Delta$
1	$^1\text{A}(\text{Mn}^{\text{V}})^{[b]}$	$(\delta^2 a_{1u}^2 a_{2u}^2)$	0.0	0.0	0.0	0.0	1.557	1.953	0.602
2	$^5\text{A}_{2u}(\text{Mn}^{\text{IV}})$	$(\delta^1 \pi^{*1} \pi^{*1} a_{2u}^1)$	2.8	2.5	0.5	1.0	1.660	1.966	0.417
3	$^3\text{A}_{2u}(\text{Mn}^{\text{IV}})$	$(\delta^1 \pi^{*1} \pi^{*1} a_{2u}^1)$	3.8	2.5	0.5	-1.0	1.659	1.964	0.420
4	$^3\text{A}_{2u}'(\text{Mn}^{\text{IV}})$	$(\pi^{*1} a_{2u}^1)$	3.6	0.9	0.2	1.0	1.594	1.966	0.499
5	$^1\text{A}_{2u}'(\text{Mn}^{\text{IV}})$	$(\pi^{*1} a_{2u}^1)$	3.8	0.8	0.1	-0.9	1.589	1.965	0.509
6	$^5\text{A}_{1u}(\text{Mn}^{\text{IV}})$	$(\delta^1 \pi^{*1} \pi^{*1} a_{1u}^1)$	5.7	2.5	0.6	0.9	1.667	1.958	0.426
7	$^1\text{A}_{1u}'(\text{Mn}^{\text{IV}})$	$(\pi^{*1} a_{1u}^1)$	5.7	0.8	0.2	-1.0	1.596	1.959	0.519
8	$^3\text{A}_{1u}'(\text{Mn}^{\text{IV}})$	$(\pi^{*1} a_{1u}^1)$	6.1	0.8	0.2	1.0	1.597	1.959	0.519
9	$^3\text{A}(\text{Mn}^{\text{V}})$	$(\delta^1 \pi^{*1})$	7.5	2.4	-0.2	-0.2	1.637	1.953	0.507

[a] Bond lengths are in Å. The Mn–N bond length is the average value of the four individual values.

[b] Calculated with RODFT.

Table 2. State characterization, relative energies, group spin densities ( $\rho$ ), and critical bond parameters ( $r$ ,  $\Delta$ ) of  $[\text{MnOPor}]^+$ .<sup>[a]</sup>

Entry	Electronic configuration	Orbital occupation	$E_{\text{rel}}$ [kcal mol <sup>-1</sup> ]	$\rho_{\text{Mn}}$	$\rho_{\text{O}}$	$\rho_{\text{Por}}$	$r_{\text{MnO}}$	$r_{\text{MnN}}$ (average)	$\Delta$
1	$^3\text{A}_{1\text{u}}(\text{Mn}^{\text{IV}})$	$(\delta^1 \pi^{*1} \pi^{*1} a_{1\text{u}}^1)$	-5.9	2.5	0.6	-1.1	1.654	2.024	0.266
2	$^5\text{A}_{1\text{u}}(\text{Mn}^{\text{IV}})$	$(\delta^1 \pi^{*1} \pi^{*1} a_{1\text{u}}^1)$	-5.8	2.5	0.6	0.9	1.655	2.024	0.263
3	$^5\text{A}_{2\text{u}}(\text{Mn}^{\text{IV}})$	$(\delta^1 \pi^{*1} \pi^{*1} a_{2\text{u}}^1)$	-5.3	2.5	0.6	0.9	1.650	2.036	0.252
4	$^3\text{A}_{2\text{u}}(\text{Mn}^{\text{IV}})$	$(\delta^1 \pi^{*1} \pi^{*1} a_{2\text{u}}^1)$	-5.2	2.5	0.6	-1.1	1.650	2.036	0.254
5	$^3\text{A}_{1\text{u}}(\text{Mn}^{\text{IV}})$	$(\pi_{\text{xz}}^{*1} a_{1\text{u}}^1)$	-1.9	1.0	0.0	1.0	1.590	2.024	0.342
6	$^1\text{A}(\text{Mn}^{\text{V}})$	$(\delta^2 a_{1\text{u}}^2 a_{2\text{u}}^2)$	0.0	0.0	0.0	0.0	1.541	2.002	0.416

[a] Bond lengths are in Å. The Mn–N bond length is the average value of the four individual values.

Table 3. State characterization, relative energies, group spin densities ( $\rho$ ), and critical bond parameters ( $r$ ,  $\Delta$ ) of  $[\text{MnOPorH}_2\text{O}]^+$ .<sup>[a]</sup>

Entry	Electronic configuration	Orbital occupation	$E_{\text{rel}}$ [kcal mol <sup>-1</sup> ]	$\rho_{\text{Mn}}$	$\rho_{\text{O}}$	$\rho_{\text{Por}}$	$\rho_{\text{H}_2\text{O}}$	$r_{\text{MnO}}$	$r_{\text{Mn-OH}_2}$	$r_{\text{MnN}}$ (average)	$\Delta$
1	$^3\text{A}_{2\text{u}}(\text{Mn}^{\text{IV}})$	$(\delta^1 \pi^{*1} \pi^{*1} a_{2\text{u}}^1)$	-13.2	2.3	0.8	-1.1	0.0	1.661	2.177	2.040	0.122
2	$^5\text{A}_{2\text{u}}(\text{Mn}^{\text{IV}})$	$(\delta^1 \pi^{*1} \pi^{*1} a_{2\text{u}}^1)$	-13.2	2.4	0.7	0.9	0.0	1.662	2.177	2.041	0.119
3	$^3\text{A}_{1\text{u}}(\text{Mn}^{\text{IV}})$	$(\delta^1 \pi^{*1} \pi^{*1} a_{1\text{u}}^1)$	-10.8	2.3	0.8	-1.1	0.0	1.664	2.200	2.029	0.125
4	$^5\text{A}_{1\text{u}}(\text{Mn}^{\text{IV}})$	$(\delta^1 \pi^{*1} \pi^{*1} a_{1\text{u}}^1)$	-10.2	2.4	0.7	0.9	0.0	1.661	2.210	2.030	0.137
5	$^1\text{A}(\text{Mn}^{\text{V}})$	$(\delta^2 a_{1\text{u}}^2 a_{2\text{u}}^2)$	0.0	0.0	0.0	0.0	0.0	1.535	2.223	2.009	0.268

[a] Bond lengths are in Å. The Mn–N bond length is the average value of the four individual values.

The lowest electronic state of the corrole analogue **1** (Table 1, entry 1) is  $^1\text{A}(\text{Mn}^{\text{V}})$ , that is a singlet state with doubly occupied  $\delta$ ,  $a_{1\text{u}}$  and  $a_{2\text{u}}$  orbitals and two empty  $\pi^*$  orbitals. In contrast, the ground states of **2** and **3** possess a high-spin manganese(IV) ion whose electrons are coupled to the porphyrin radical in either a ferro- or antiferromagnetic fashion (Tables 2 and 3). The corresponding quintet and triplet states are virtually (but accidentally) identical in energy. Interestingly, while in **2** the most stable  $^3,^5\text{A}_{1\text{u}}(\text{Mn}^{\text{IV}})$  states with a single  $a_{1\text{u}}$  electron are quite close in energy to the  $^3,^5\text{A}_{2\text{u}}(\text{Mn}^{\text{IV}})$  states, in **3** the lowest states are  $^3,^5\text{A}_{2\text{u}}(\text{Mn}^{\text{IV}})$ , which are well separated from the  $^3,^5\text{A}_{1\text{u}}(\text{Mn}^{\text{IV}})$  states. In other words the sixth ligand in **3** has a significant effect on the ordering of the  $a_{1\text{u}}$  and  $a_{2\text{u}}$  orbitals.

The trends in the Mn–O bond lengths in Tables 1–3 support the variation in the occupation of the  $\pi_{\text{MnO}}^*$  orbitals. For instance, the  $^1\text{A}(\text{Mn}^{\text{V}})$  state of **1** has two empty  $\pi^*$  orbitals and a short Mn–O bond length of 1.557 Å (Table 1, entry 1). With one electron in a  $\pi^*$  orbital this value increases to 1.59 Å (Table 1, entries 4, 5) and with two triplet-coupled  $\pi^*$  electrons the bond length becomes 1.66 Å (Table 1, entries 2, 3). The other geometric features are the displacement,  $\Delta$ , of the manganese atom relative to the plane of the macrocycle, and the average Mn–N distance. Clearly,  $\text{MnO}(\text{Cor})$  has the largest  $\Delta$  and the shortest Mn–N distance.<sup>[14]</sup> In all spin states, we also note that these values change significantly. For example, the  $^1\text{A}(\text{Mn}^{\text{V}})$  states of **1**, **2**, and **3** have large  $\Delta$  values and short Mn–N bonds, which are apparently essential for the stabilization of  $^1\text{A}(\text{Mn}^{\text{V}})$ .

Another evident trend in the Tables 1–3 is the tendency of manganese to prefer wherever possible high-spin situations. Thus for example, in **2** (Table 2, entries 1, 2) the  $^3,^5\text{A}_{1\text{u}}(\text{Mn}^{\text{IV}})$  states with  $\delta^1 \pi^{*1} \pi^{*1} a_{1\text{u}}^1$  occupation are lower by about 4 kcal mol<sup>-1</sup> than  $^3\text{A}_{1\text{u}}'(\text{Mn}^{\text{IV}})$  with  $\delta^2 \pi^{*1} \pi^{*0} a_{1\text{u}}^1$  occupation

(Table 2, entry 5). This known effect<sup>[2d]</sup> originates in the large d–d exchange stabilization of the small manganese atom, and is expected to play an important role in determining the identity of the ground state of the complex.

The salient features of Tables 1–3 are summarized in Figure 1, which depicts the relationship of the lowest lying states for the three systems, in terms of a state correlation diagram. To highlight the state reversals, we define arbitrarily as zero the energy of the  $^1\text{A}$  state. The first change appears as we move from the five-coordinate corrole complex **1** to the corresponding porphyrin complex **2**. Thus, in **1** the closed shell  $^1\text{A}(\text{Mn}^{\text{V}})$  situation is the ground state, while the high-spin  $^5\text{A}_{2\text{u}}(\text{Mn}^{\text{IV}})$  and  $^5\text{A}_{1\text{u}}(\text{Mn}^{\text{IV}})$

are excited states. The corrole → porphyrin replacement reverses the order and establishes  $^5\text{A}_{1\text{u}}(\text{Mn}^{\text{IV}})$  as the ground state, whereas  $^1\text{A}(\text{Mn}^{\text{V}})$  lies significantly higher in energy. Adding a water molecule as an axial ligand reverses the  $^3,^5\text{A}_{1\text{u}}(\text{Mn}^{\text{IV}})$ – $^3,^5\text{A}_{2\text{u}}(\text{Mn}^{\text{IV}})$  ordering, making the latter the ground state. The  $^1\text{A}(\text{Mn}^{\text{V}})$  state is still a high-lying excited state. Thus, unlike the situation in  $\text{MnOCor}$  which stabilizes the  $\text{Mn}^{\text{V}}$  state, in  $[\text{MnOPor}]^+$  with and without a sixth ligand the  $\text{Mn}^{\text{V}}$  is an excited state. We shall now try to explain these features.

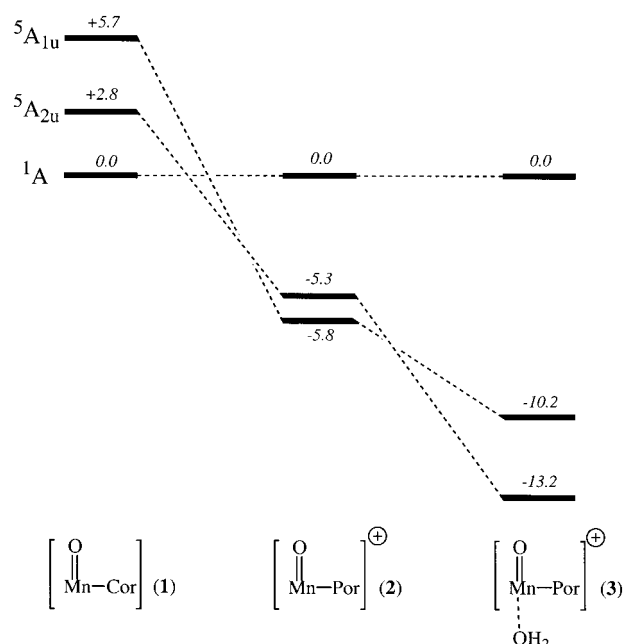


Figure 1. State correlation for the  $^1\text{A}(\text{Mn}^{\text{V}})$ ,  $^5\text{A}_{2\text{u}}(\text{Mn}^{\text{IV}})$ , and  $^5\text{A}_{1\text{u}}(\text{Mn}^{\text{IV}})$  in **1**, **2**, and **3**. The zero is arbitrarily defined as the  $^1\text{A}$  energy in each case.

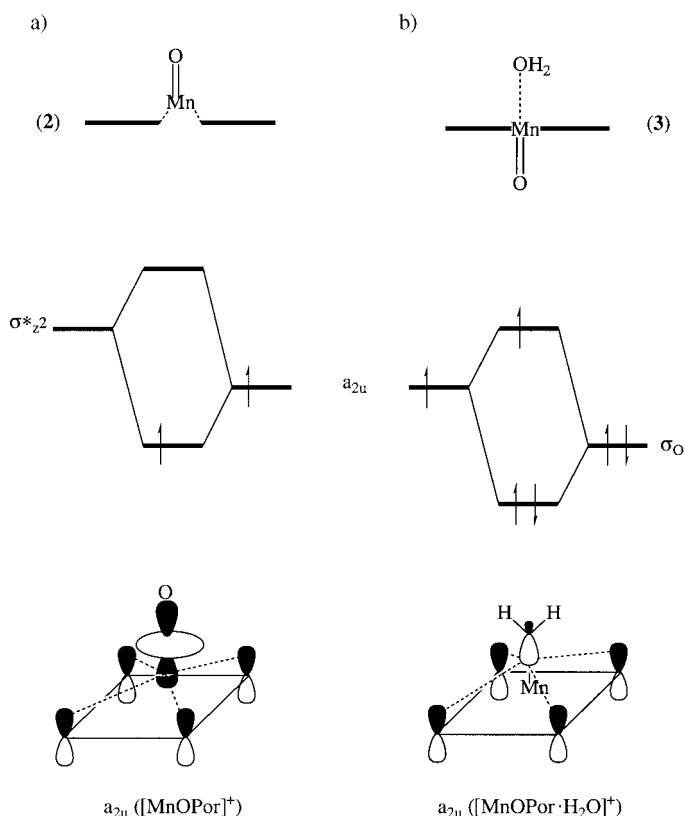
A few factors conspire to make MnOCor an  $^1A(Mn^V)$  ground state, as opposed to  $[MnOPor]^+$  that has an  $^{3,5}A_{1u}(Mn^{IV})$  ground state. One factor is orbital energy, which tends to prefer closed shell states, and the other one is the d–d exchange stabilization that is large for manganese and prefers high-spin situations.<sup>[2d]</sup>

The orbital energy factor is associated with the displacement of the manganese atom relative to the plane of the porphyrin or corrole ring. This displacement enables the mixing between the  $\pi^*_{MnO}$  orbitals and the in-plane bonding “ $e_u$ ” orbitals of the porphyrin or corrole rings. In fact, inspection of the  $\pi^*_{MnO}$  orbitals in Schemes 1 and 2 reveals this mixing, and shows that the  $\pi^*_{MnO}$  orbitals involve antibonding interactions with the  $\sigma$  lobes of the “ $e_u$ ” orbitals.

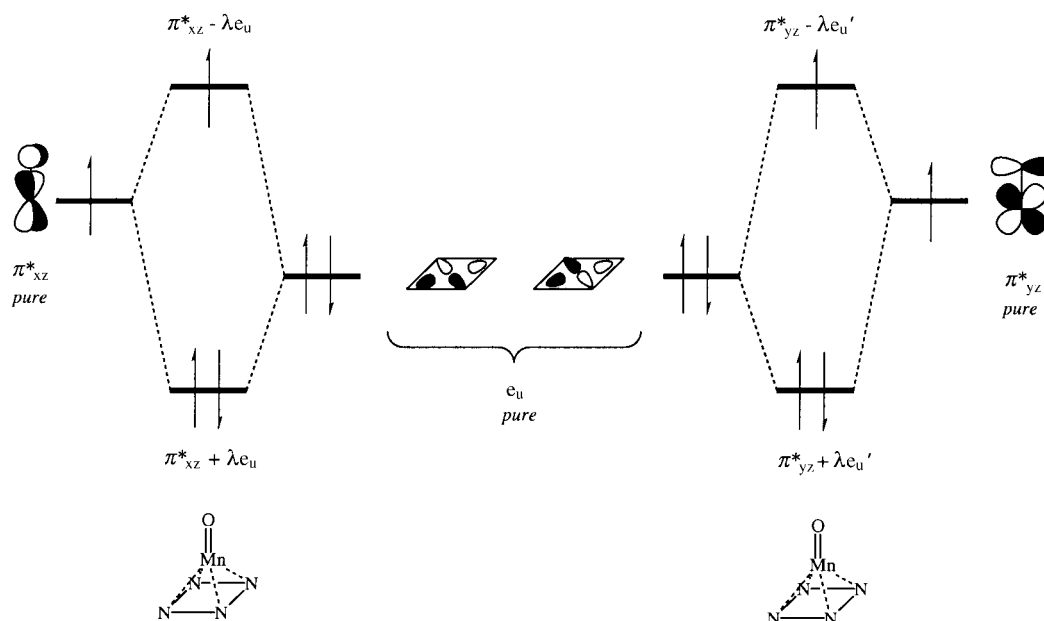
To understand the outcome of this mixing we reconstruct it in Scheme 3 from the pure fragment orbitals:  $\pi^*(\text{pure})$  and  $e_u(\text{pure})$ . The  $e_u(\text{pure})$  orbitals are lower lying since they are involved in Mn–N bonding.<sup>[15]</sup> By mixing with  $\pi^*(\text{pure})$ , the  $e_u$  orbitals acquire an increased bonding character ( $\lambda$  is the mixing coefficient). This strengthens and shortens the Mn–N bonds. In contrast the  $\pi^*$  orbitals acquire antibonding character and are therefore raised in energy. To begin with, due to the smaller bite of corrole compared with porphyrin, MnO(Cor) will have a large  $\Delta$ .<sup>[16]</sup> Consequently, the interactions in Scheme 3 will be stronger in MnO(Cor) than in  $[MnOPor]^+$ . It follows therefore, that MnO(Cor) will have shorter Mn–N bonds, larger  $\Delta$ , and higher  $\pi^*$  orbitals, than  $[MnOPor]^+$ .

Clearly, the orbital energy factor will disfavor occupancy in the  $\pi^*$  orbitals, and will favor a  $\delta^2\pi^0a_{1u}^2a_{2u}^2$  occupation. This orbital energy effect will compete with the d–d exchange stabilization that prefers  $\delta^1\pi^1\pi^1a_{1u}^2a_{2u}^1$ . In MnOCor the  $\pi^*$  orbitals are raised sufficiently to override the exchange stabilization leading to a  $^1A(Mn^V)$  ground state. In  $MnOPor^+$ , the  $\pi^*$  orbitals are not raised as much and the exchange stabilization wins over, and favors the  $\delta^1\pi^1\pi^1a_{1u}^1a_{2u}^2$  ( $^{3,5}A_{1u}$ ) state over the  $^1A(Mn^V)$  state.

Let us discuss now the ligand effect on  $[MnOPor]^+$ . Adding a water molecule to  $[MnOPor]^+$  is seen to stabilize the  $^{3,5}A_{2u}(Mn^{IV})$  states, while the  $^1A(Mn^V)$  state lies now 13.2 kcal mol<sup>−1</sup> higher (Figure 1, Table 3). The reason for this is the following. In the absence of a sixth ligand, the manganese atom is pulled off plane with respect to the ring (Scheme 4). This can be seen



Scheme 4. a) Orbital mixing of  $a_{2u}$  with  $\sigma^*_{z^2}$ , and resulting  $a_{2u}$  orbital in  $[MnOPor]^+$ . b)  $\sigma_O$ - $a_{2u}$  orbital mixing and resulting  $a_{2u}$  orbital in  $[MnOPor \cdot H_2O]^+$ .



Scheme 3. Mixing of the “pure”  $e_u$  pair with the “pure”  $\pi^*$  orbitals to produce bonding and antibonding combinations;  $\lambda$  is the mixing coefficient.

by comparing the  $\Delta$  values in Tables 2 and 3 where the  $[\text{MnOPor}]^+$  states have larger  $\Delta$  values than those with the water complex. Since the Mn atom is hanging off the plane with a rather large displacement  $\Delta$ , the empty  $\sigma_{z^2}^*$  virtual orbital can mix with the occupied  $a_{2u}$  orbital (these orbitals have in fact an identical symmetry label in all point groups equal or lower than  $C_{4v}$ ) and stabilize it as shown in Scheme 4a, which highlights the interaction along the Mn–O axis at the bottom. This orbital mixing lowers the  $a_{2u}$  orbital below the  $a_{1u}$  orbital that remains unaffected. Consequently,  $a_{2u}$  gets doubly occupied and  ${}^3,5A_{1u}(\text{Mn}^{\text{IV}})$  becomes the ground state in  $[\text{MnOPor}]^+$ .

Adding a water ligand to the system will pull the manganese atom more into the plane of the porphyrin ring (smaller  $\Delta$  values) and at  $\Delta \approx 0$  the  $\sigma_{z^2}^* - a_{2u}$  interaction is turned off. Furthermore, it is replaced by an antibonding interaction with the  $\sigma$ -oxygen lone pair that raises the  $a_{2u}$  orbital (Scheme 4b). The destabilization of  $a_{2u}$  lowers the  ${}^3,5A_{2u}(\text{Mn}^{\text{IV}})$  states in which the orbital is singly occupied. Since the  $a_{1u}$  orbital is not affected, the  ${}^3,5A_{1u}(\text{Mn}^{\text{IV}})$  states in which  $a_{2u}$  is doubly occupied are now higher lying compared with the situation in  $[\text{MnOPor}]^+$  (see Figure 1).

We conclude that the preference for  $[\text{Mn}^{\text{IV}}\text{OPor}^{+}]$  over  $[\text{Mn}^{\text{V}}\text{OPor}]$  does not change with the addition of a sixth ligand to porphyrin. At least for water, six-coordination disfavors the singlet even more. Calculations (BPW91) by Ghosh and Gonzalez<sup>[10a]</sup> indicate that electronegative ligands like  $\text{F}^-$  may assist in achieving a  ${}^1A(\text{Mn}^{\text{V}})$  ground state. Our results indicate that  $\text{Mn}^{\text{V}}\text{O}$  is going to be difficult to stabilize. Indeed as shown by Groves et al.,<sup>[2f]</sup> it takes positively charged porphyrin substituents like *ortho*-pyridilium to stabilize a singlet  $\text{PorMn}^{\text{V}}\text{O}$  state. With corrole, this situation is the ground state already for the pristine system.

## Conclusion

Corrole complexes have an inherent propensity for  $\text{Mn}^{\text{V}}\text{O}$ , while the porphyrin complexes prefer  $\text{Mn}^{\text{IV}}\text{O}$  states.<sup>[8]</sup> This difference is shown to originate owing to a combination of short Mn–N bonds and large Mn out-of-plane displacements in the corrole, which lead to quite unexpected interactions of the  $\text{Mn}=\text{O} \pi^*$  orbitals with the in-plane orbitals of the corrole. Although experimental confirmation for oxo–manganese complexes is still lacking, we note that in the highly relevant oxo–chromium(v) corrole all these effects have been seen: large  $\Delta$ , short metal–N bonds, and significant unpaired spin density on the nitrogen atoms.<sup>[16]</sup> The intriguing question that remains to be resolved is how the spin-state preference affects catalysis in its two most important aspects; reactivity and selectivity. The existing results with both porphyrins and corroles suggest that the reactivity of singlet oxo–manganese(v) complexes is surprisingly low.<sup>[2, 5]</sup> How this phenomenon could affect selectivity will be addressed in a forthcoming investigation by a combination of computational and experimental approaches.

## Acknowledgements

The research was sponsored by the Israel Academy of Sciences [SS (444/99-2); ZG (368-00)], and in part by the Ministry of Science, Sport and Culture (SS). FO thanks the EU for a Marie Curie Fellowship.

- [1] a) *The Porphyrin Handbook* (Eds.: K. M. Kadish, K. M. Smith, R. Guilard), Academic Press, San Diego, **2000**; b) D. Mansuy, P. Battioni in *The Porphyrin Handbook*, Vol. 4 (Eds.: K. M. Kadish, K. M. Smith, R. Guilard), Academic Press, San Diego, **2000**, Chapter 26, p. 1; c) J. T. Groves, K. Shalyaev, J. Lee in *The Porphyrin Handbook*, Vol. 4 (Eds.: K. M. Kadish, K. M. Smith, R. Guilard), Academic Press, San Diego, **2000**, Chapter 27, p. 17; d) K. S. Suslick in *The Porphyrin Handbook*, Vol. 4 (Eds.: K. M. Kadish, K. M. Smith, R. Guilard), Academic Press, San Diego, **2000**, Chapter 28, p. 28; e) Y. Watanabe in *The Porphyrin Handbook*, Vol. 4 (Eds.: K. M. Kadish, K. M. Smith, R. Guilard), Academic Press, San Diego, **2000**, Chapter 30, p. 97.
- [2] a) J. T. Groves, W. J. Kruper, R. C. Haushalter, *J. Am. Chem. Soc.* **1980**, *102*, 6375; b) J. T. Groves, M. K. Stern, *J. Am. Chem. Soc.* **1987**, *109*, 3812; c) J. T. Groves, M. K. Stern, *J. Am. Chem. Soc.* **1988**, *110*, 8628; d) R. S. Czernuszewicz, Y. O. Su, M. K. Stern, K. A. Macor, D. Kim, J. T. Groves, T. G. Spiro, *J. Am. Chem. Soc.* **1988**, *110*, 4158; e) J. T. Groves, J. Lee, S. S. Marla, *J. Am. Chem. Soc.* **1997**, *119*, 6269; f) N. Jin, J. T. Groves, *J. Am. Chem. Soc.* **1999**, *121*, 2923; g) N. Jin, J. L. Bourassa, S. C. Tizio, J. T. Groves, *Angew. Chem.* **2000**, *112*, 4007; *Angew. Chem. Int. Ed.* **2000**, *39*, 3849.
- [3] a) A. Sorokin, A. Robert, B. Meunier, *J. Am. Chem. Soc.* **1993**, *115*, 7293; b) J. Bernadou, A.-S. Fabiano, A. Robert, B. Meunier, *J. Am. Chem. Soc.* **1994**, *116*, 9375.
- [4] a) T. J. Collins, R. D. Powell, C. Slebodnick, E. S. Uffelman, *J. Am. Chem. Soc.* **1990**, *112*, 899; b) J. P. Collman, J. I. Brauman, P. D. Hampton, H. Tanaka, D. S. Bohle, R. T. Hembre, *J. Am. Chem. Soc.* **1990**, *112*, 7980.
- [5] a) Z. Gross, G. Golubkov, L. Simkhovich, *Angew. Chem. Int. Ed.* **2000**, *39*, 4045; b) J. Bendix, I. J. Dmochowski, H. B. Gray, A. Mahammed, L. Simkhovich, Z. Gross, *Angew. Chem.* **2000**, *112*, 4214; *Angew. Chem. Int. Ed.* **2000**, *39*, 4048.
- [6] a) W. Adam, V. R. Stegmann, C. R. Saha-Möller, *J. Am. Chem. Soc.* **1999**, *121*, 1879; b) W. Adam, C. Mock-Knoblach, C. R. Saha-Möller, M. Herderich, *J. Am. Chem. Soc.* **2000**, *122*, 9685.
- [7] E. N. Jacobsen, *Acc. Chem. Res.* **2000**, *33*, 421.
- [8] We use the common oxidation state formalism, which enables the simplest rationalization of the d-block occupancy. In this formalism the oxidation state and charge of the ligand is determined by the number of electrons it “takes” from the metal center to complete its valence shell to octet. Thus the porphyrin ring is 2–, while corrole is 3–. The oxo ligand is 2–, while water has an oxidation state of zero. A porphyrin ring with a  $\pi$ -radical cation state has a mixed situation; it is 2– in the  $\sigma$  frame and +1 in the  $\pi$  system. Thus, for neutral complex  $\text{MnOCor}$ , in which Mn appears as  $\text{Mn}^{\text{IV}}$ , the corrole must appear as a cation radical. In contrast, for the same complex with  $\text{Mn}^{\text{V}}$ , the corrole has a closed shell. There exist other electron counting schemes, for example ones which assign  $\text{O}^{-1}$  for high-spin situations, or one which describes  $[\text{Mn}^{\text{IV}}\text{OCor}]^{+}$  as having a formal  $\text{Mn}^{\text{V}}$  center. These other schemes are not used here.
- [9] a) M. Filatov, N. Harris, S. Shaik, *J. Chem. Soc. Perkin Trans. 2* **1999**, 399; b) M. Filatov, N. Harris, S. Shaik, *Angew. Chem.* **1999**, *111*, 3730; *Angew. Chem. Int. Ed.* **1999**, *38*, 3510; c) F. Ogliaro, S. Cohen, M. Filatov, S. Shaik, *Angew. Chem. Int. Ed.* **2000**, *112*, 4009; *Angew. Chem. Int. Ed.* **2000**, *39*, 3851; d) F. Ogliaro, S. P. de Visser, J. T. Groves, S. Shaik, *Angew. Chem. Int. Ed.* **2001**, *113*, 2858; *Angew. Chem. Int. Ed.* **2001**, *40*, 2874.
- [10] a) A. Ghosh, E. Gonzalez, *Isr. J. Chem.* **2000**, *40*, 1; b) A. Ghosh, T. Wondimagenen, A. B. J. Parusel, *J. Am. Chem. Soc.* **2000**, *122*, 5100.
- [11] Jaguar 4.1, Schrödinger, Inc., Portland, Oregon, **2001**.
- [12] A. Ricca, C. W. Bauschlicher, *Chem. Phys. Lett.* **1995**, *245*, 150.
- [13] M. Filatov, S. Shaik, *J. Phys. Chem. A* **1998**, *102*, 3835.
- [14] It is worthwhile to mention the out-of-plane displacements observed in isolated pentacoordinate complexes, 0.29 Å in a manganese(III) and 0.42 and 0.43 Å in two manganese(IV) complexes. See: a) J. Bendix,

- H. B. Gray, G. Golubkov, Z. Gross, *Chem. Commun.* **2000**, 1957; b) G. Golubkov, J. Bendix, H. B. Gray, A. Mahammed, I. Goldberg, A. J. DiBilio, Z. Gross, *Angew. Chem.* **2001**, *113*, 2190; *Angew. Chem. Int. Ed.* **2001**, *40*, 2132.
- [15] a) K. Tatsumi, R. Hoffmann *Inorg. Chem.* **1981**, *20*, 3771; b) K. Tatsumi, R. Hoffmann, *J. Am. Chem. Soc.* **1981**, *103*, 3328.
- [16] A. E. Meier-Callahan, H. B. Gray, Z. Gross, *Inorg. Chem.* **2000**, *39*, 3605.

Received: June 19, 2001 [F3351]